PAPER

Highly efficient Yb:YAG microchip laser for direct generation of radially polarized vector vortices

Engineering Research Express

CrossMark

PAPER

Highly efficient Yb:YAG microchip laser for direct generation of radially polarized vector vortices

Dimeng Chen, Shu Cai and Jun Dong (ORCID)

Laboratory of Laser and Applied Photonics (LLAP), Department of Electronic Engineering, School of Electronic Science and Engineering, Xiamen University, Xiamen, People's Republic of China

E-mail: jdong@xmu.edu.cn

Abstract

High beam quality, highly efficient radially polarized vector vortex beam has been generated in a Yb:YAG microchip laser pumped with an annular beam formed with a hollow focus lens. The output power of 2.15 W has been achieved at the absorbed pump power of 3.53 W. The optical-to-optical efficiency is 60.9%. The radially polarized vector vortex lasers working at 1030 nm, 1050 nm, 1030/1050 nm dual-wavelength depending on applied pump power. High polarization purity with degree of polarization of over 91% has been achieved for radially polarized vector vortex lasers. Our work provides an effective method for developing compact wavelength tunable, radially polarized vector vortex lasers.

1. Introduction

Cylindrical vector (CV) beams are laser beams with cylindrical symmetry in polarization [1] and have found applications in high resolution imaging, nanoparticle manipulation, laser machining, remote sensing. Radially polarized laser beam is one of distinguished CV beams and has unique tightly focusing property [2, 3]. Radially polarized beams have been widely used in optical trapping [4–7], optical tweezers [8], material processing [9–12], nonlinear dynamic [13], formation of vortex arrays [14], and so on. Various methods such as using photonic crystal grating [15], Brewster angle prism [16] have been proposed to generate radially polarized beams in solid state lasers. Radially and azimuthally polarized beams in a Yb:YAG laser have been obtained by inserting a birefringent crystal and intra-cavity lens in the laser cavity [17]. However, inserting extra optical modulation elements in laser cavity makes the laser complex and degrades the optical efficiency and beam quality. Annular-beams have been widely used to pump solid-state lasers to generate vector vortices with various polarization states including radial and azimuthal polarization states. Annular-beams are usually formed by using an axicon [18] or mode conversion fiber [19]. Radially polarized beam was generated in a Yb:YAG thin-disk laser pumped by a ring-shaped beam formed with hollow optical fiber components [20]. Polarization states tunable Laguerre–Gaussian (LG$_{0,1}$) vector-vortex beams were generated in a Yb:YAG microchip laser pumped with an annular beam directly formed in a fiber-coupled laser-diode [21]. However, the conversion efficiency is low when an annular beam is shaped from a laser-diode with Gaussian distribution. There are severe coupling and diffraction losses during the beam shaping processing. Recently, an annular beam has been efficiently formed with a hollow focus lens (HFL) [22]. HFL provides a very effective method to produce focused annular-beam with high optical efficiency. Vector vortices switching from radial polarization to azimuthal polarization have been achieved in a Nd:YAG microchip laser pumped with an annular beam formed with a HFL. 0.8 W radially polarized laser and 1.16 W azimuthally polarized laser have been achieved. The optical efficiency of 11.6% is low because there is severe thermal effect and low quantum efficiency of Nd:YAG crystal. Yb:YAG crystal has been demonstrated to be an efficient laser material because it has lots of excellent characteristics such as broad absorption bandwidth, small quantum defect, long lifetime, broad emission bandwidth [23]. Compact radially polarized vector vortex lasers are extremely needed for various applications. By applying an annular beam formed with a HFL as a pump

Figure 1. Schematic of the Yb:YAG microchip laser for generating radially polarized vector-vortex beam, CL is the collimating lens, HFL is the hollow focus lens, *r* is the radius of curvature of the negative meniscus lens, Δz is the distance between focal spot and the rear cavity mirror, OC is the output coupler.
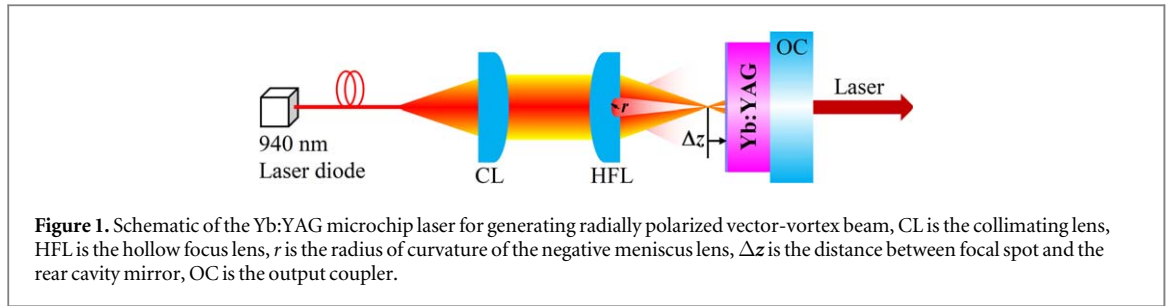
beam, Yb:YAG microchip laser should be an effective solution for generating radially polarized beam, and needed to be investigated.

In this paper, we demonstrated a highly efficient, radially polarized vector-vortex Yb:YAG microchip laser pumped with an annular beam formed with a HFL. Output power of 2.15 W has been obtained at the absorbed pump power of 3.53 W and the optical efficiency is as high as 60.9%. The degree of polarization has been measured to be over 91% for radially polarized vector-vortex beams. The pump power dependent wavelength tunable radially polarized vector-vortex lasers working at 1030 nm, 1050 nm, and 1030/1050 nm dual-wavelength have been demonstrated.
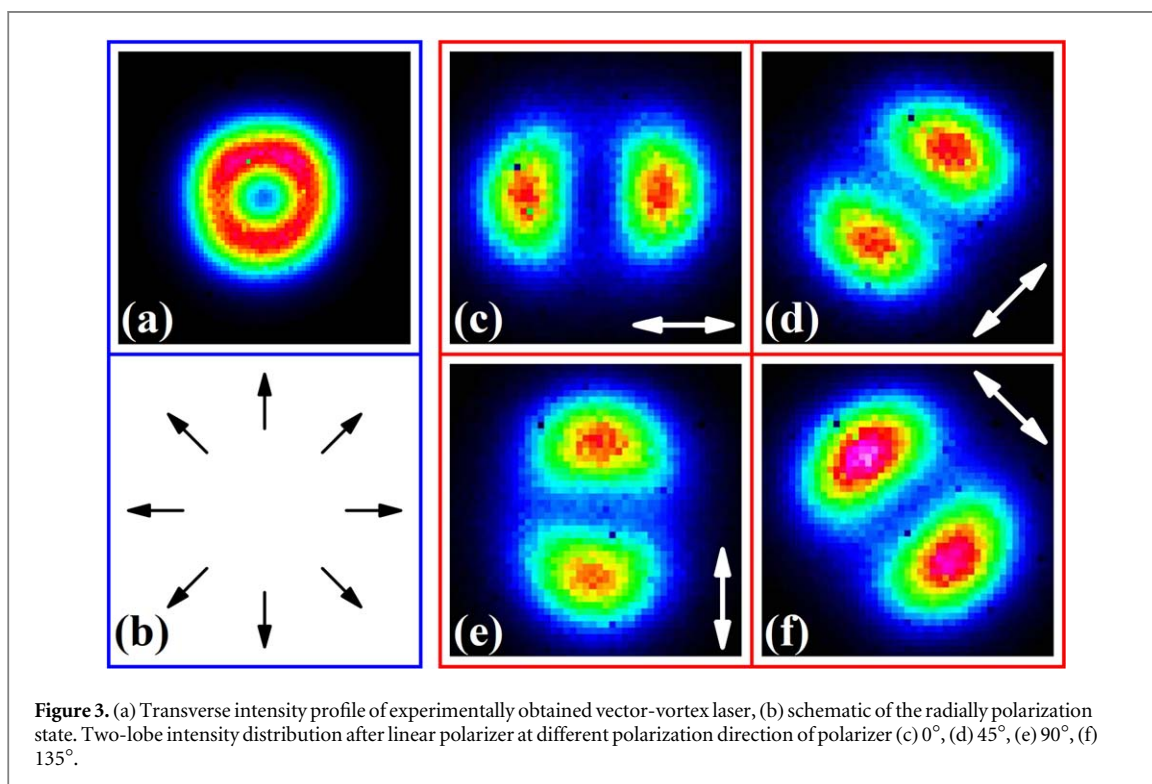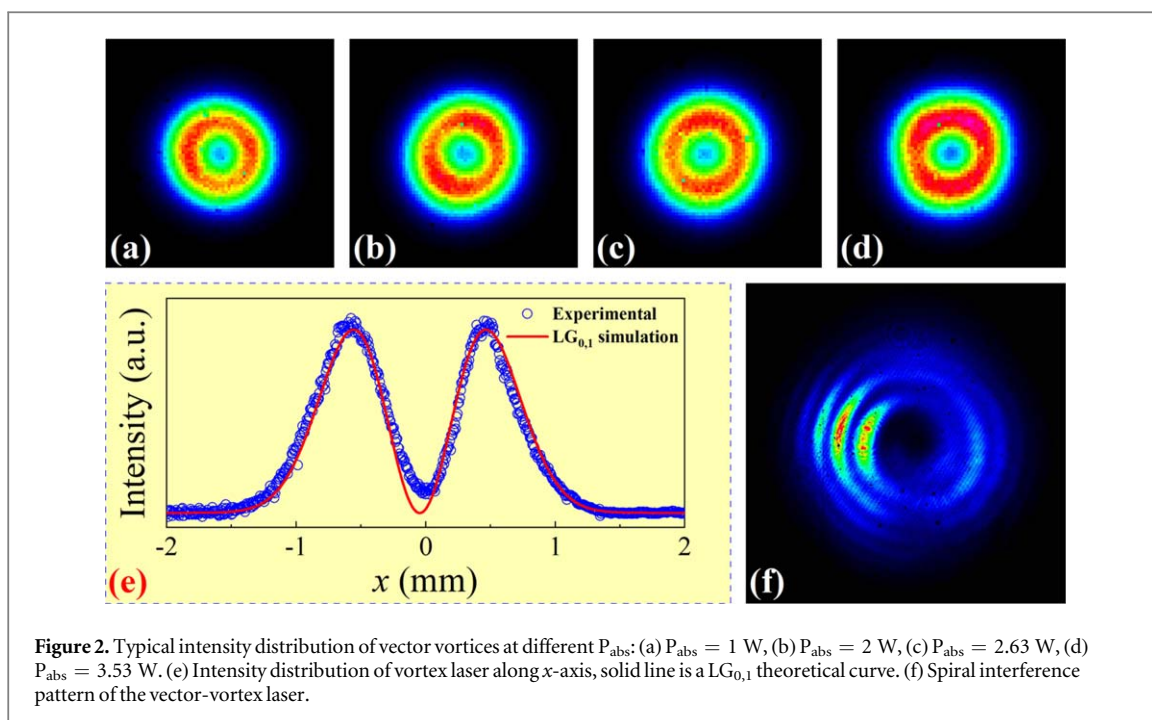
2. Experiment

The experimental setup of generating radially polarized vector-vortex beams in an annular beam pumped Yb:YAG microchip laser is shown in figure 1. The pump source is a 940 nm fiber-coupled laser diode (core diameter: 200 μm, numerical aperture: 0.22). The pump light emitting from the fiber was collimated with a collimating lens (CF) with 8 mm focal length. The collimated beam was focused with a home-made HFL (8 mm focal length). According to [22] and [24], the HFL is made of D-LaK6 glass, the diameter of the HFL is 10 mm, the radius of curvature (*r*) and the diameter of the negative meniscus lens are 0.5 mm and 1 mm (see supplementary material (available online at stacks.iop.org/ERX/2/045035/mmedia)). Thus, an annular beam was formed away from the focal spot. The diameter of 120 μm was measured at focal spot. The microchip laser is constructed with a 10 at.% Yb:YAG crystal thin plate (1.2 mm thick) and a plane output coupler (OC). The reflectivity of the OC is 95% at 1030 nm. The rear cavity mirror is formed with a coating of high reflection (>99%) at 1030 nm. The radially polarized vector vortices were generated by positioning rear cavity mirror of the microchip laser 0.2 mm away from the focal spot. The laser experiments were carried out at ambient temperature. The output power was measured with a Thorlabs PM100D power meter. A Thorlabs BC106-VIS beam profile analyzer was used to monitor and record the laser transverse field distribution.

3. Results and discussion

Under annular beam pumping condition, the absorbed pump power (P_{abs}) of the Yb:YAG microchip laser was evaluated by measuring the incident pump power and the residual power before and after Yb:YAG crystal, respectively. The pump power absorption efficiency was 53% independent on the incident pump power. When P_{abs} reached 0.65 W, the Yb:YAG microchip laser oscillated and the output beam profiles were doughnut shape. The laser transverse intensity profile is maintained doughnut with increase in the P_{abs}. Figures 2(a)–(d) show some typical measured intensity distributions of the doughnut-shaped lasers at different P_{abs}. The experimentally obtained doughnut profile along *x*-axis, as shown in figure 2(e), was fitted well with $LG_{0,1}$ expression, which clearly confirmed that the obtained doughnut-shaped intensity profiles at different P_{abs} were $LG_{0,1}$ mode laser. Oscillation of $LG_{0,1}$ mode laser was attributed to good mode matching between annular pump beam formed with HFL and $LG_{0,1}$ laser mode in Yb:YAG microchip laser. The helical wavefronts of the obtained doughnut mode lasers at different P_{abs} were measured with a Mach–Zehnder interferometer. A tiny beam was selected from vortex laser with an aperture and focused with a lens to form the spherical wave reference beam, then interfered with the doughnut mode laser beam. It is clearly seen in figure 2(f) that the resultant interference pattern has a clear anticlockwise spiral fringe. The anticlockwise spiral interference pattern is maintained at different P_{abs} once the laser oscillates. Evidently, these results verify that the doughnut-shaped lasers are $LG_{0,1}$ vortex laser with stable helical handness.

A linear polarized was used to measure the states of polarization of the experimentally obtained vortex lasers at different P_{abs}. Two-lobe transverse intensity patterns were observed when a vortex laser with intensity profile as shown in figure 3(a) passed through a linear polarizer. As shown figure 3(c), horizontal symmetrical two-lobe

Figure 2. Typical intensity distribution of vector vortices at different P_{abs}: (a) $P_{abs} = 1$ W, (b) $P_{abs} = 2$ W, (c) $P_{abs} = 2.63$ W, (d) $P_{abs} = 3.53$ W. (e) Intensity distribution of vortex laser along x-axis, solid line is a $LG_{0,1}$ theoretical curve. (f) Spiral interference pattern of the vector-vortex laser.

Figure 3. (a) Transverse intensity profile of experimentally obtained vector-vortex laser, (b) schematic of the radially polarization state. Two-lobe intensity distribution after linear polarizer at different polarization direction of polarizer (c) $0°$, (d) $45°$, (e) $90°$, (f) $135°$.

pattern was obtained when the polarization direction of the linear polarizer was set horizontally (e.g. the polarizer direction is set to $0°$). As shown in figure 3(d), two-lobe pattern was rotated $45°$ clockwise as the linear polarizer was rotated $45°$ clockwise. Two-lobe pattern was rotated synchronically with the further rotation of the linear polarizer, as indicated in figures 3(e) and (f). Rotation of two-lobe pattern with the linear polarizer in the same speed and direction clearly proves that the experimentally generated doughnut vortex laser is radially polarized. The state of polarization of radially polarized beam is schematically shown in figure 3(b). The radial polarization state is maintained for the vortex beams within the range of available pump power. The oscillation of radially polarized mode in this plane-parallel microchip laser is caused by the thermally induced bifocusing effect. Under the annular beam pumping, the temperature gradient formed in Yb:YAG crystal induces different thermal focal lengths for radial and azimuthal polarized components. The optical path difference (OPD) for
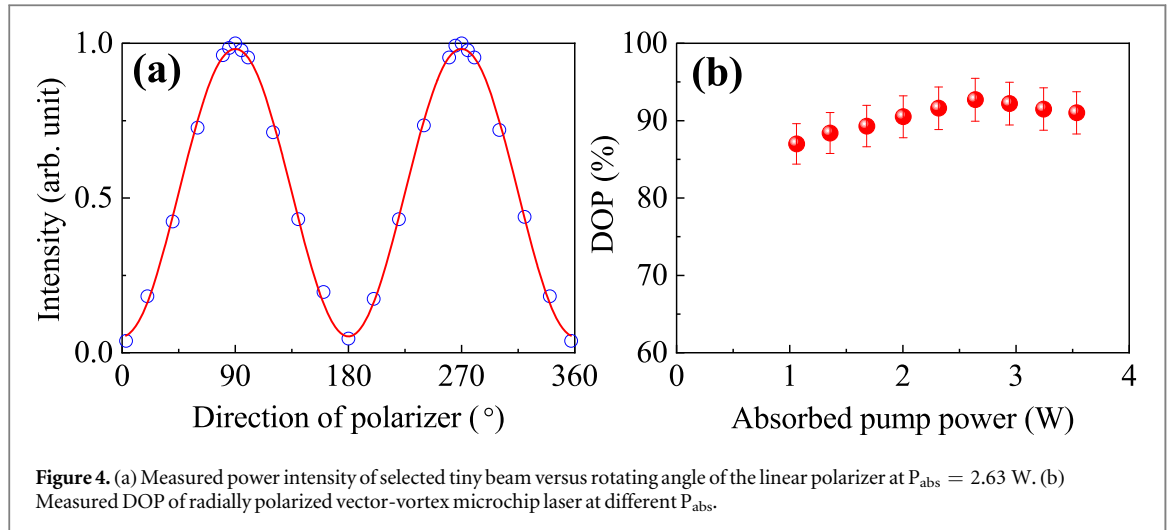
Figure 4. (a) Measured power intensity of selected tiny beam versus rotating angle of the linear polarizer at $P_{abs} = 2.63$ W. (b) Measured DOP of radially polarized vector-vortex microchip laser at different P_{abs}.

radially polarized component of $LG_{0,1}$ mode is larger than that for azimuthally polarized component [19]. The effective heat generation in Yb:YAG crystal is less than that in Nd:YAG crystal because there is only one third of heat generated in Yb:YAG laser compared to that generated in Nd:YAG laser [25]. Therefore, the localized oscillating laser spot size of radial polarized component is well overlapped with localized pump region spot size, which is beneficial to radially polarized component oscillating in Yb:YAG microchip laser [22]. Therefore, only radially polarized vortex laser was obtained in the current available pump power.

The polarization purity of the radially polarized vector-vertex beams was evaluated by measuring the degree of polarization (DOP) at different P_{abs}. It is well known that state of polarization of any tiny local laser beam is linear for a pure radially polarized laser. Therefore, an aperture with a diameter about 200 μm was placed 1 m away from the output coupler to randomly select a small portion from the vector vortex beam. By passing a linear polarizer, the power intensity of selected beam was measured by rotating the polarizer. Figure 4(a) gives the variation of the measured power intensity as a function of rotating angel of the polarizer at $P_{abs} = 2.63$ W. The variation of the power intensity with polarizer rotating angle was fitted well with the function of square of sine, which provides a solid evidence for that the selected small beam is linearly polarized. The DOP of the local tiny beam can be expressed with $(I_{max} - I_{min})/(I_{max} + I_{min})$, where I_{max} and I_{min} are the maximum and minimum power intensity obtained from the fitting curve. Therefore, based on the fitting power intensity parameters in figure 4(a), the DOP was determined to be 92.7% at $P_{abs} = 2.63$ W. The DOP of the vector vortex laser beams at different P_{abs} was plotted in figure 4(b). The DOP increases from 87% to 92.7% when the P_{abs} increases from 1 W to 2.63 W, and then slightly decreases to 91% at available maximum P_{abs} of 3.53 W. The slight change of the DOP with P_{abs} may be attributed to the linearly polarized components competition and thermal effect induced depolarization effect. The DOP of over 91% at high pump power level suggests that the good polarization purity is achieved in the radially polarized Yb:YAG microchip laser.

The propagation property of the radially polarized vector-vortex beams was evaluated by measuring the beam radii along the propagation direction. Figure 5 shows the variation of the beam radius of the vector vortex beam as a function of the propagation position at $P_{abs} = 3.53$ W. The variation of the beam radius along x-axis and y-axis is nearly identical at different positions, which proves that the perfect symmetrical intensity distribution of radially polarized vector vortex beam. The beam quality factor along x-axis, M_x^2 and along y-axis, M_y^2 were fitted to be 2.22 and 2.24, which are very close to the theoretical beam quality factor of 2 for an ideal $LG_{0,1}$ laser mode. High beam quality with M^2 less than 2.3 has been achieved for experimentally obtained radially polarized vector-vortex beam.

The laser spectra of the radially polarized Yb:YAG microchip laser were analyzed at different P_{abs} with an Anritsu optical spectral analyzer (MS9740A), and some typical laser spectra are shown in figure 6. The multi-longitudinal-mode oscillation is dominant owing to the broad emission spectrum of Yb:YAG crystal and high gain achieved under high pump power intensity. The laser started to oscillate when the P_{abs} was higher than 0.65 W. The laser oscillated at 1030 nm when the P_{abs} was less than 2.1 W. The longitudinal mode increases with the P_{abs}. One example of laser spectrum at 1030 nm is shown in figure 6(a). At $P_{abs} = 2$ W, laser oscillates in nine longitudinal modes. Further increase P_{abs} up to 2.1 W, the 1050 nm laser starts to oscillate, therefore, 1030/1050 nm dual-wavelength laser is achieved. Nine longitudinal modes for 1030 nm laser and two longitudinal modes with wide separation for 1050 nm oscillate at $P_{abs} = 2.3$ W, as shown in figure 6(b). The 1030/1050 nm dual-wavelength laser oscillation is maintained when P_{abs} is increased upon to 3.1 W. However, for the dual-wavelength laser oscillation, the longitudinal-mode intensity and number at 1030 nm and 1050 nm change in
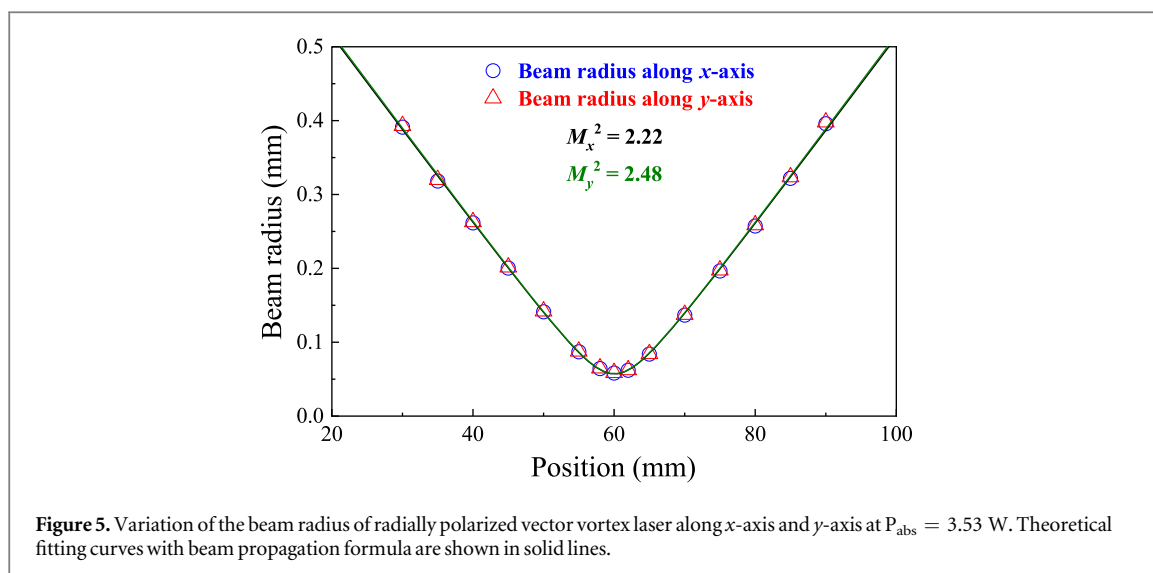
Figure 5. Variation of the beam radius of radially polarized vector vortex laser along *x*-axis and *y*-axis at $P_{abs} = 3.53$ W. Theoretical fitting curves with beam propagation formula are shown in solid lines.
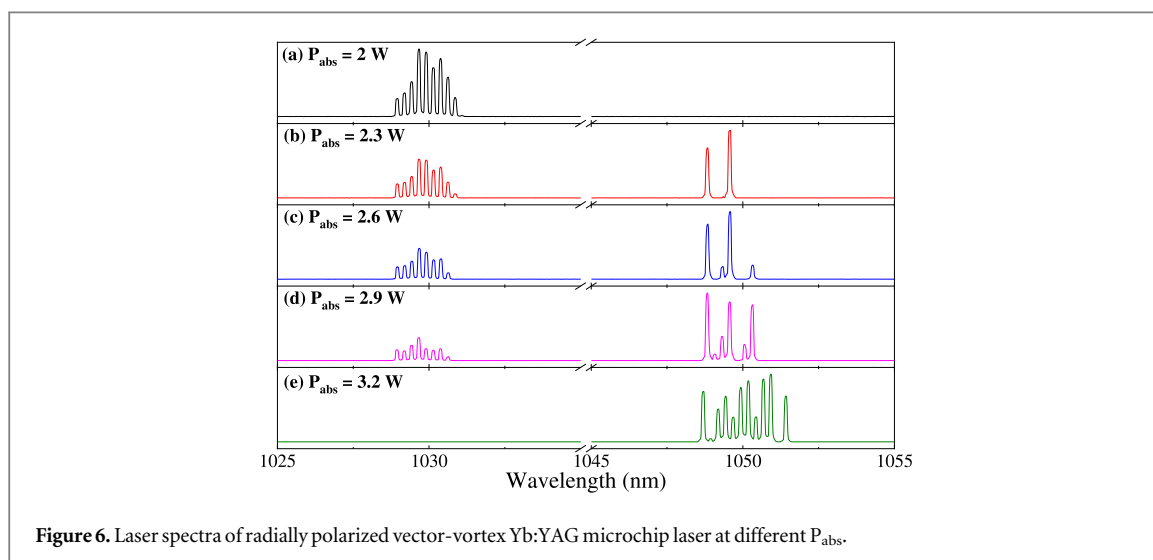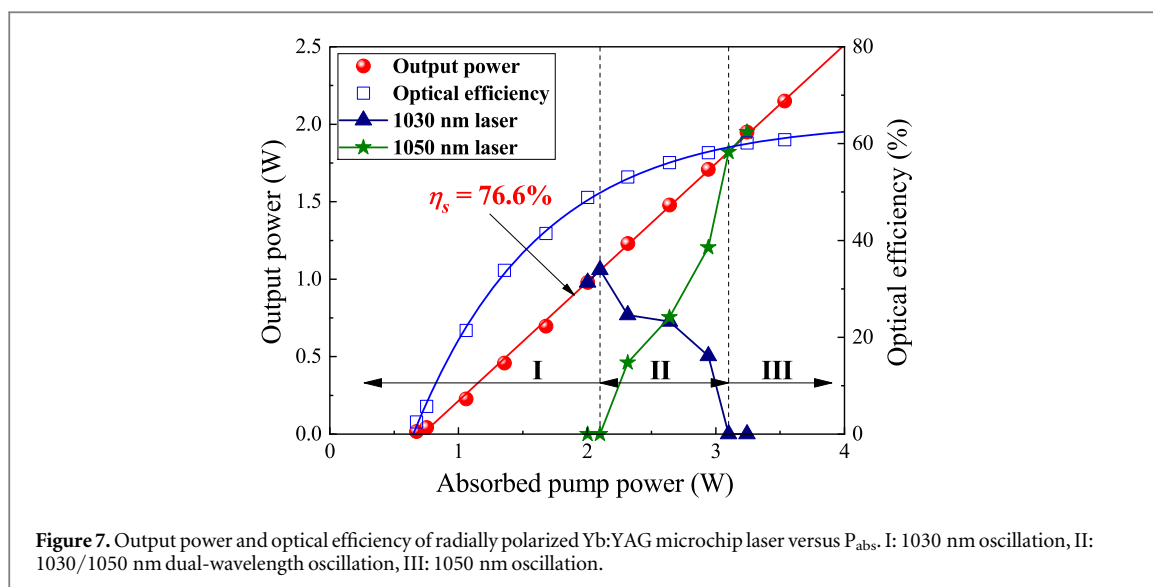

Figure 6. Laser spectra of radially polarized vector-vortex Yb:YAG microchip laser at different P_{abs}.

the opposite way with P_{abs}, as shown in figures 6(b)–(d). The 1030 nm laser disappears when the P_{abs} is increased to 3.1 W, and only 1050 nm laser oscillates when the P_{abs} is higher than 3.1 W, as shown in figure 6(e). As indicated in figure 6, by adjusting pump power, the radially polarized vector-vortex laser can oscillate at 1030 nm, 1050 nm, and 1030/1050 nm dual-wavelength. Thus, we demonstrate pump power-dependent wavelength tunable radially polarized vector-vortex lasers. Laser wavelength switching from 1030 to 1050 nm is controlled by the local temperature rise induced thermal population at low laser level for 1030 nm radiation [26]. Besides high Q cavity formed with an OC of 95% reflectivity, the oscillating wavelength in Yb:YAG microchip laser is mainly governed by the reabsorption loss at 1030 nm. Temperature has great effect on the absorption spectrum of Yb:YAG crystal. The working temperature of Yb:YAG microchip laser under annular beam pumping was estimated and found that the temperature of Yb:YAG crystal increases linearly with incident pump power. The temperature of about 45° was estimated at the incident pump power of 6.7 W. The reabsorption at 1030 nm becomes severe with rise of temperature. Therefore, the threshold pump power increases for 1030 nm laser oscillation; while the pump power induced local temperature has less effect on the threshold pump power for 1050 nm radiation. For Yb:YAG crystal as a gain medium, the emission cross section at 1050 nm laser transition is only one fifth of that at 1030 nm, however, enhanced reabsorption at 1030 nm with temperature rise degrades the net gain for 1030 nm laser oscillation. Thus, the oscillating wavelength of Yb:YAG laser is determined by the reabsorption loss of 1030 nm transition. The local temperature increases with incident pump power, laser emission at 1030 nm is suppressed by the increased reabsorption loss, and the laser prefers to oscillate at 1050 nm.

Figure 7 shows the output power and the optical-to-optical efficiency as a function of P_{abs}. The absorbed pump power required for laser oscillation is 0.65 W. With P_{abs} increasing, the linear increase of output power

Figure 7. Output power and optical efficiency of radially polarized Yb:YAG microchip laser versus P_{abs}. I: 1030 nm oscillation, II: 1030/1050 nm dual-wavelength oscillation, III: 1050 nm oscillation.

with a slope efficiency of 76.6% suggests that output power of the radially polarized vortex laser can be further scaled. Output power is 2.15 W when the P_{abs} is 3.53 W. The corresponding optical-to-optical efficiency is about 60.9%. The optical efficiency is 32% with respect to the incident pump power of 6.7 W. From the laser spectra of radially polarized vortex microchip laser (figure 6), we can see that there are three absorbed pump power regions for achieving vortex laser oscillation at different wavelengths. 1030 nm laser oscillates at $P_{abs} < 2.1$ W, 1050 nm laser oscillates at $P_{abs} > 3.1$ W, while 1030/1050 nm dual-wavelength radially polarized vortex laser oscillates within a wide pump power range (about 1 W from 2.1 to 3.1 W). The output power of dual-wavelength laser varies from 1 W to 1.8 W, as shown in figure 7. The output power of 1030 nm laser and 1050 nm laser in dual-wavelength laser were estimated by evaluating the laser emitting spectra and found the contribution of 1030 nm laser decreased and the contribution of 1050 nm laser increased with P_{abs} for the dual-wavelength laser oscillation, as shown in figure 7. Pump power-dependent 1030/1050 nm dual-wavelength lasers with relative contribution of 1030 nm laser and 1050 nm laser have potential applications in terahertz wave generation, optical communication, laser sensing, digital holography, and so on. The highest output powers at 1030 nm and 1050 nm are 1 W and 2.15 W for radially polarized vortex lasers, respectively. Therefore, pump power-dependent wavelength switchable radially polarized vortex laser has been demonstrated under an HFL formed annular beam pumping.

The optical efficiency increases rapidly with P_{abs} when P_{abs} is less than 2.3 W, then increases slowly with further increase P_{abs}. The highest optical efficiency of 60.9% was achieved at $P_{abs} = 3.53$ W. No saturation effect of the optical efficiency was observed under current available pump power, which suggests that the performance of the radially polarized vortex Yb:YAG microchip laser can be enhanced at high pump power. Compare to the performance of Nd:YAG microchip laser pumped with an annular beam formed with a HFL [22], the output power (2.15 W) was doubled, and optical efficiency (32% with respect to the incident pump power) was tripled. Excellent beam matching between $LG_{0,1}$ mode laser and high power intensity annular beam formed with a HFL is main mechanism for generating radially polarized vortices in highly efficient Yb:YAG microchip laser. For an annular beam with a focus spot of 120 μm in diameter, the incident pump power intensity is about 60 kW cm^{-2} at incident pump power of 6.7 W. Accounting to the theoretical model of temperature tuning Yb:YAG microchip laser [27], such high pump power intensity is sufficient for Yb:YAG microchip laser achieving efficient laser oscillation at room temperature.

4. Conclusion

In conclusion, high beam quality, highly efficient, radially polarized vector-vortex lasers with tunable laser wavelengths have been demonstrated in a Yb:YAG microchip laser pumped with an annular beam formed with a hollow focus lens. The output power is 2.15 W when the P_{abs} is 3.53 W. The optical efficiency is as high as 60.9%. High polarization purity with DOP of over 91% is achieved for radially polarized vector-vortex microchip laser. High beam quality has been achieved with M^2 less than 2.3 in radially polarized Yb:YAG microchip laser. Pump power-dependent wavelength switchable, radially polarized vector-vortex lasers oscillate at 1.03 μm to 1.05 μm, and 1.03/1.05 μm dual-wavelength. Annular beam formed with a HFL has been demonstrated to be an effective pumping scheme for developing highly efficient radially polarized vector-vortex Yb:YAG microchip laser, which

provides more flexible choice for potential applications such as material processing, high resolution imaging and quantum computation.

Acknowledgments

ORCID iDs

Jun Dong   https://orcid.org/0000-0001-7072-5435

References

[1] Zhan Q W 2009 Cylindrical vector beams: from mathematical concepts to applications *Adv. Opt. Photonics* **1** 1–57
[2] Dorn R, Quabis S and Leuchs G 2003 Sharper focus for a radially polarized light beam *Phys. Rev. Lett.* **91** 4233901
[3] Lerman G M and Levy U 2008 Effect of radial polarization and apodization on spot size under tight focusing conditions *Opt. Express* **16** 4567–81
[4] Kuga T, Torii Y, Shiokawa N, Hirano T, Shimizu Y and Sasada H 1997 Novel optical trap of atoms with a doughnut beam *Phys. Rev. Lett.* **78** 4713–6
[5] Zhan Q W 2004 Trapping metallic Rayleigh particles with radial polarization *Opt. Express* **12** 3377–82
[6] Kawauchi H, Yonezawa K, Kozawa Y and Sato S 2007 Calculation of optical trapping forces on a dielectric sphere in the ray optics regime produced by a radially polarized laser beam *Opt. Lett.* **32** 1839–41
[7] Zhou Z H, Zhang Y L and Zhu L Q 2016 Theoretical and experimental studies on optical trapping using radially polarized beams *Opt. Quantum Electron.* **48** 10 404
[8] Nieminen T A, Heckenberg N R and Rubinsztein-Dunlop H 2008 Forces in optical tweezers with radially and azimuthally polarized trapping beams *Opt. Lett.* **33** 122–4
[9] Niziev V G and Nesterov A V 1999 Influence of beam polarization on laser cutting efficiency *J. Phys. D-Appl. Phys.* **32** 1455–61
[10] Venkatakrishnan K and Tan B 2012 Generation of radially polarized beam for laser micromachining *J. Laser Micro Nanoeng.* **7** 274–8
[11] Rutkauskas M, Farrell C, Dorrer C, Marshall K L, Crawford T, Lundquist T R, Vedagarbha P, Erington K, Bodoh D and Reid D T 2016 Two-photon laser-assisted device alteration in CMOS integrated circuits using linearly, circularly and radially polarized light *Microelectron. Reliab.* **60** 62–6
[12] Drevinskas R, Zhang J Y, Beresna M, Gecevicius M, Kazanskii A G, Svirko Y P and Kazansky P G 2016 Laser material processing with tightly focused cylindrical vector beams *Appl. Phys. Lett.* **108** 5221107
[13] Okulov A Y 2020 Structured light entities, chaos and nonlocal maps *Chaos Solitons Fractals* **133** 109638
[14] Okulov A Y 2008 3D-vortex labyrinths in the near field of solid-state microchip laser *J. Mod. Opt.* **55** 241–59
[15] Li J L, Ueda K, Zhong L X, Musha M, Shirakawa A and Sato T 2008 Efficient excitations of radially and azimuthally polarized Nd^{3+}: YAG ceramic microchip laser by use of subwavelength multilayer concentric gratings composed of Nb_2O_5/SiO_2 *Opt. Express* **16** 10841–8
[16] Kozawa Y and Sato S 2005 Generation of a radially polarized laser beam by use of a conical brewster prism *Opt. Lett.* **30** 3063–5
[17] Thirugnanasambandam M P, Senatsky Y and Ueda K 2011 Generation of radially and azimuthally polarized beams in Yb:YAG laser with intra-cavity lens and birefringent crystal *Opt. Express* **19** 1905–14
[18] Wei M D, Lai Y S and Chang K C 2013 Generation of a radially polarized laser beam in a single microchip Nd:YVO$_4$ laser *Opt. Lett.* **38** 2443–5
[19] Fang Z Q, Xia K G, Yao Y and Li J L 2014 Radially polarized LG$_{01}$-mode Nd:YAG laser with annular pumping *Appl. Phys. B-Lasers Opt.* **117** 219–24
[20] Dietrich T, Rumpel M, Graf T and Ahmed M A 2015 Investigations on ring-shaped pumping distributions for the generation of beams with radial polarization in an Yb:YAG thin-disk laser *Opt. Express* **23** 26651–9
[21] Chen D M, Wang X C, He H S and Dong J 2019 Vector vortices with tunable polarization states directly generated in a microchip laser *Appl. Phys. Express* **12** 052012
[22] He H S, Chen Z and Dong J 2017 Direct generation of vector vortex beams with switchable radial and azimuthal polarizations in a monolithic Nd:YAG microchip laser *Appl. Phys. Express* **10** 052701
[23] Dong J, Bass M, Mao Y L, Deng P Z and Gan F X 2003 Dependence of the Yb^{3+} emission cross section and lifetime on temperature and concentration in yttrium aluminum garnet *J. Opt. Soc. Am. B-Opt. Phys.* **20** 1975–9
[24] Dong J and He H 2016 A hollow focus lens for directing generating hollow focused beam *People's Republic of China patent* ZL20161111338.3(in Chinese)
[25] Fan T Y 1993 Heat generation in Nd:YAG and Yb:YAG *IEEE J. Quantum Electron.* **29** 1457–9
[26] Dong J, Ueda K and Kaminskii A A 2010 Laser-diode pumped efficient Yb:LuAG microchip lasers oscillating at 1030 and 1047 nm *Laser Phys. Lett.* **7** 726–33
[27] Dong J and Ueda K 2005 Temperature-tuning Yb:YAG microchip lasers *Laser Phys. Lett.* **2** 429–36